

## Electronic Supplementary Information

### A combination of an organic alloy and a heterojunction towards a rod-tail helix architecture with dual-color-emitting properties

Hongyang Zhang,<sup>a,b</sup> Haitao Wang,<sup>b</sup> Peng-Cheng Qian,<sup>\*c</sup> and Wai-Yeung Wong<sup>\*a,b</sup>

<sup>a</sup>Department of Applied Biology and Chemical Technology, The Hong Kong Polytechnic University, Hung Hom, Hong Kong, China.

<sup>b</sup>Department of Chemistry, Hong Kong Baptist University, Waterloo Road, Hong Kong, China

<sup>c</sup>Key Laboratory of Environmental Functional Materials Technology and Application of Wenzhou City, Institute of New Materials & Industry, College of Chemistry & Materials Engineering, Wenzhou University, Wenzhou 325035, China.

**Materials.** BA and BN were purchased from Sigma-Aldrich, and used without further treatment. For the solvents, tetrahydrofuran (A.R.) and ethanol (A.R.) were purchased from RCI Labscan Ltd., Thailand. Ultrapure water with a resistivity of 18.2 MΩ•cm at 25 °C was produced by using a Milli-Q apparatus of Milipore Corporation.

**Synthesis of BA microrods and BN microtubes.** 1D BA microrods were synthesized by a liquid-phase self-assembly route. In a typical synthesis, 1 mL of a stock solution of BA in THF (5 mM) was rapidly injected into 5 mL of a 4:1 (v/v) ethanol/H<sub>2</sub>O mixture at room temperature and the mixture was allowed to stand for 10 min, afterwards a yellow suspension was formed. Similarly, 1D BN microtubes were prepared by adding 1 mL of a stock solution of BN in THF (2.5 mM) into 5 mL of a 4:1 (v/v) ethanol/H<sub>2</sub>O mixture. The resultant colloidal samples were collected on the surface of a quartz substrate. In the meantime, part of the flocculent colloid was separated by centrifugation at 3500 rpm and washed several times with ultrapure water, and finally dried under vacuum for further analysis.

**Synthesis of BA<sub>0.72</sub>BN<sub>0.28</sub> helical microribbons.** In the same condition, 1 mL of a stock solution of BA/BN in THF with mol/mol = 2:1 ( $C_{BA} = 5$  mM,  $C_{BN} = 2.5$  mM) was rapidly injected into 5 mL of a 4:1 (v/v) ethanol/H<sub>2</sub>O mixture at room temperature, and the mixture was allowed to stand for 10 min. Consequently a

brownish black suspension was formed, the resultant colloidal samples were collected on the surface of a quartz substrate and dried under vacuum for further analysis.

**Synthesis of BA@BA<sub>0.72</sub>BN<sub>0.28</sub> core-shell structures via a stepwise growth process.** During this process, the as-prepared BA microrods acted as the seed and dispersed under the synthetic condition for those assemblies (v/v = 4:1 ethanol/H<sub>2</sub>O solvent mixture, 5 mL), followed by fast injection of 1 mL stock solution of BA/BN in THF with a 2:1 molar ratio ( $C_{BA} = 5$  mM,  $C_{BN} = 2.5$  mM) and gentle shaking of the mixed solution. Within 10 min, the BA<sub>0.72</sub>BN<sub>0.28</sub> microribbons would be formed and grown on the surface of BA microrods. As a result, a large number of core-shell structures, BA@BA<sub>0.72</sub>BN<sub>0.28</sub>, were synthesized in the system. The resultant colloidal samples were collected on the surface of a quartz substrate and dried under vacuum for further analysis.

**Characterization.** The morphologies and sizes of the as-prepared samples were examined by utilizing field-emission scanning electron microscopy (LEO 1530 Field Emission SEM) at acceleration voltages of 20 kV. Prior to measurement, the as-prepared samples were coated with a thin gold layer using a SPI Module Sputter Coater. TEM photographs were obtained by means of a Tecnai G2 20 S-TWIN Transmission Electron Microscope operated at 120 or 200 kV. The samples were prepared by depositing one drop of colloidal dispersion on a carbon-coated copper grid, and dried at room temperature under high vacuum. The crystal structure characterizations of these as-synthesized assemblies were performed via PXRD on a Bruker AXS D8 Advance X-Ray Diffractometer, with Cu K $\alpha$  (Running condition: 40 kV, 40 mA) for analyzing the composition and phase purity. The fluorescence microscopic photographs were taken by using a Leica DMRBE fluorescence microscopy with the aid of a spot-enhanced charged couple device (CCD, Diagnostic Instrument, Inc.) and the samples were prepared by dropping the dispersion (100  $\mu$ L) onto a cleaned quartz slide. Laser confocal fluorescent microscopy (Leica, TCS-SP5) equipped with near ultraviolet laser (405 nm) was employed for photographing fluorescent images besides recording micro-area PL spectra of BA rod, BN tube and BA@BA<sub>0.72</sub>BN<sub>0.28</sub> rod-tail helix.

**Discussion.** Some further detailed characterizations were conducted. For 1D BA assembly, it exhibits the partial hollow rod-like morphology instead of solid or tube throughout (Fig. S1), which is related to the solvent etching mechanism,<sup>2</sup> the ethanol solvent would swap out part of the BA molecules. For the alloy BA<sub>0.72</sub>BN<sub>0.28</sub> helical ribbon, we tested its thickness by using the SEM technique, and it presents a value of 263.9 nm (Fig. S2 a). SEM analysis also reveals the formation of helical configurations including both left- and right-handed helices (Fig. S2 b), suggesting that the final product should be a racemic mixture because achiral BA and BN were used as the building blocks.<sup>3-6</sup> Besides, circular dichroism (CD) spectrum of the helical assembly was measured, which also proved that the final product should be a racemic mixture (Fig. S3). We also provided the structural analysis of BA and one alloy grown from DMF and the predicted growth morphology and direction of BA

crystal and the alloy, in which the data were obtained from the literature work<sup>1</sup> in order to support our explanation on the growth mechanism (Fig. S4). Moreover, Figure S5 presents more microscopic analyses of our fabricated BA@BA<sub>0.72</sub>BN<sub>0.28</sub> core-shell structure, no matter from the low to high magnification in the SEM images, we can see that the formation of heterostructured architecture is not a specially observed sample on a partial position, but a general phenomenon throughout the whole domain. As the thickness of heterojunction exceeds the limit of electron transmission, the TEM result is not the convincing evidence to present the core-shell dividing line, but still good for showing the specific topological configuration.

For the investigation of the  $\pi$ - $\pi$  interaction among BA and BN, we measured the emission and excitation spectra of BA, BN and BA/BN mixed solutions in different concentrations. Because it is hard to measure the excitation spectrum of the solid sample, but easy to measure that of the solution sample, we measured the emission and excitation spectra of BA solution ( $C_{\text{BA}}=10^{-4}$  mM in THF), BN solution ( $C_{\text{BN}}=10^{-4}$  mM in THF) and BA/BN precursor solution ( $C_{\text{BA}} = 5$  mM,  $C_{\text{BN}} = 2.5$  mM in THF) (Fig. S6). Firstly, we find that all the Stokes shifts are small for BA, BN and BA/BN mixed solutions, suggesting that the excitation wavelengths are close to the emission wavelengths. Secondly, the bathochromic effect of concentration is remarkable, as we can see the emission wavelength of BA/BN precursor solution ( $C_{\text{BA}} = 5$  mM,  $C_{\text{BN}} = 2.5$  mM in THF) is longer than that of the  $10^{-4}$  mM THF solutions of both BA and BN. This indicates that the  $\pi$ - $\pi$  interaction is the main interaction among these  $\pi$ -conjugated molecules. Thirdly, for BA/BN precursor solution, we can see the emission is blue shifted relative to the emission of the solid BA/BN helix. That is because the  $\pi$ - $\pi$  interaction is stronger in the solid form compared to that in the solution form, which cause the red shift of the emission spectra. We further explored the effect of  $\pi$ - $\pi$  interaction on the emission in the solution sample. We measured the the PL spectra of BA and BN (mol/mol = 2:1) mixed THF solutions in different concentrations (Fig. S7), and the results show the superposition of the PL spectra of BA and BN at the low concentration. Then, we increased the concentration as far as  $C_{\text{BA}} = 5$  mM and  $C_{\text{BN}} = 2.5$  mM in THF. We can find the obvious energy transfer (ET) from BA to BN, the emission peak of BA is gradually reduced and the main peak of BN is red shifted from 575 nm to 605 nm, indicating the strong  $\pi$ - $\pi$  interaction within BA and BN.

## References:

1. Y. Lei, Y. Sun, Y. Zhang, H. Zhang, H. Zhang, Z. Meng, W. Y. Wong, J. Yao, H. Fu, *Nat. Commun.* 2018, **9**, 4358.
2. Y. Lei, Y. Jin, D. Y. Zhou, W. Gu, X. B. Shi, L. S. Liao, S. T. Lee, *Adv. Mater.* 2012, **24**, 5345–5351.
3. T. G. Barclay, K. Constantopoulos, J. Matison, *Chem. Rev.* 2014, **114**, 10217–10291.
4. M. H. Liu, L. Zhang, T. Y. Wang, *Chem. Rev.* 2015, **115**, 7304–7397.
5. Y. Wang, J. Xu, Y. W. Wang, H. Y. Chen, *Chem. Soc. Rev.* 2013, **42**, 2930–2962.

6. S. Srivastava, A. Santos, K. Critchley, K. S. Kim, P. Podsiadlo, K. Sun, J. Lee, C. Xu, G. D. Lilly, S. C. Glotzer, N. A. Kotov, *Science* **2010**, *327*, 1355–1359.

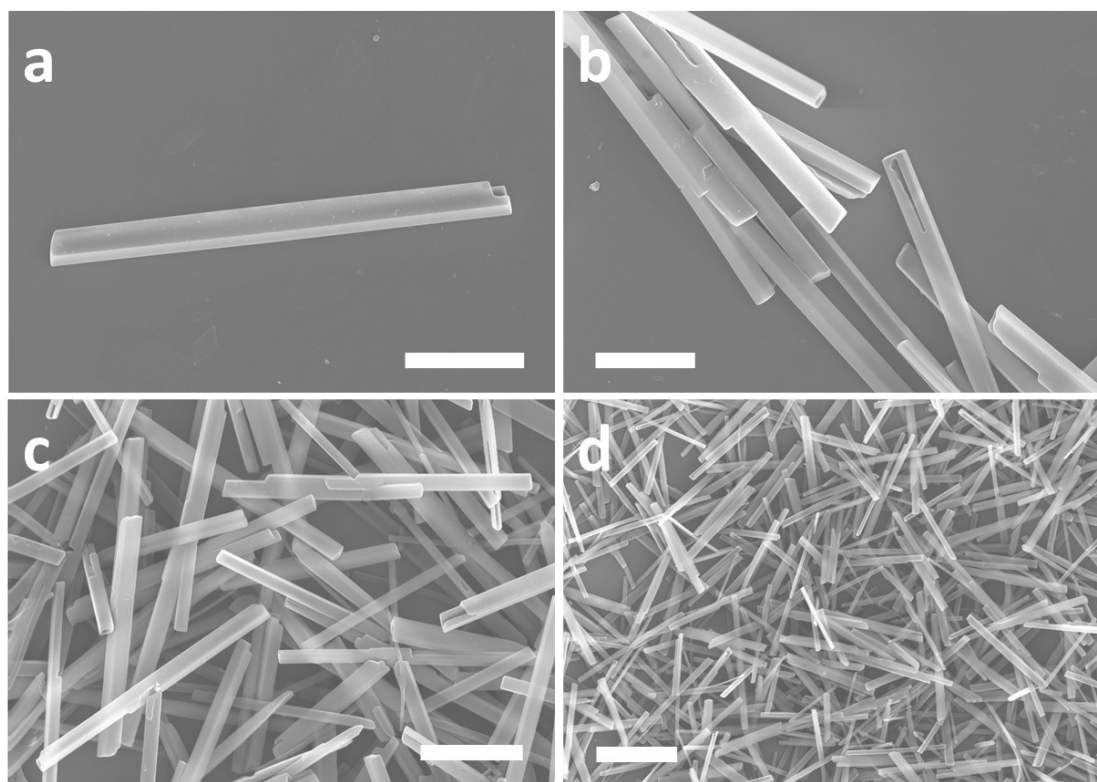


**Figure S1.** SEM images of the 1D BA assembly prepared by adding a stock solution of pure BA in THF (5mM, 1 mL) into a 5 mL of ethanol/H<sub>2</sub>O mixture at v/v = 4:1. Scale bar: 10  $\mu\text{m}$  in **a**, **b** and 20  $\mu\text{m}$  in **c**, **d**.

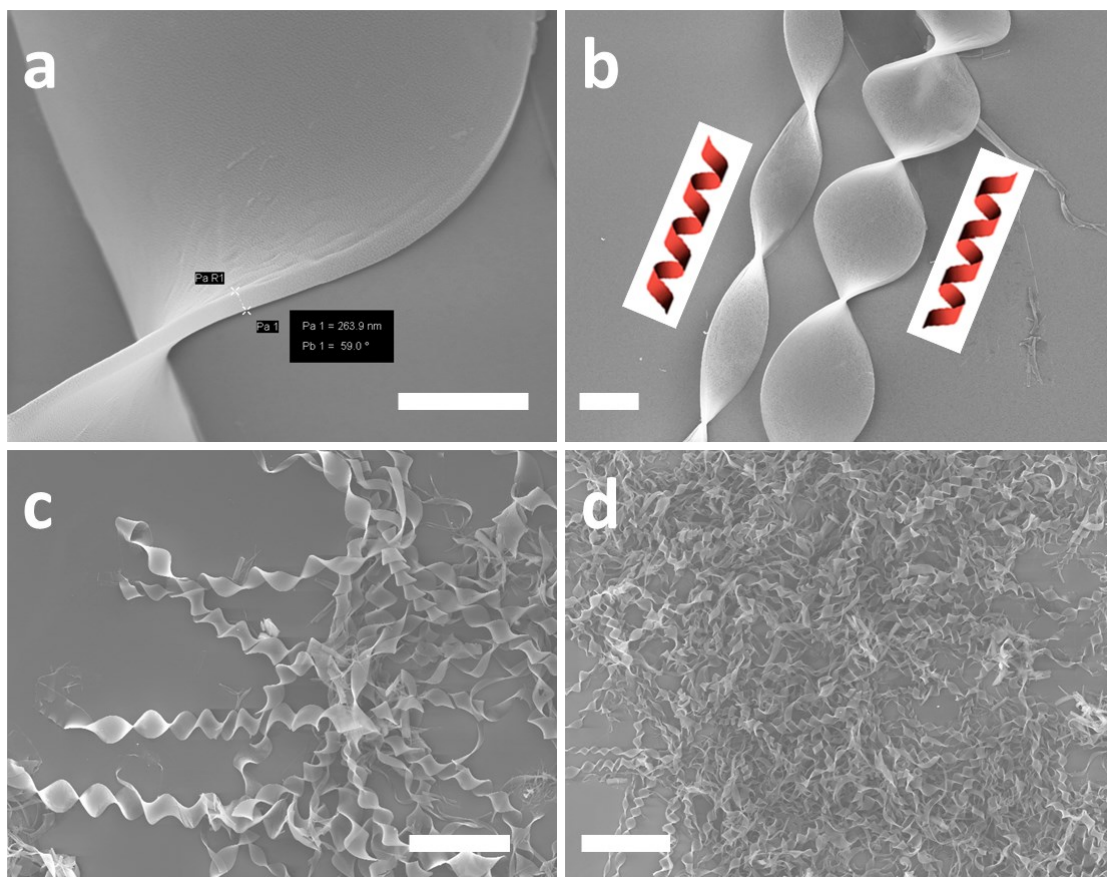


**Figure S2.** SEM images of  $BA_{0.72}BN_{0.28}$  helical ribbons prepared by adding 1 mL stock solution of BA/BN in THF with mol/mol = 2:1 ( $C_{BA} = 5 \text{ mM}$ ,  $C_{BN} = 2.5 \text{ mM}$ ) into a 5 mL of ethanol/ $H_2O$  mixture at v/v = 4:1. Scale bar: 2  $\mu\text{m}$  in **a, b** and 25  $\mu\text{m}$  in **c, d**.

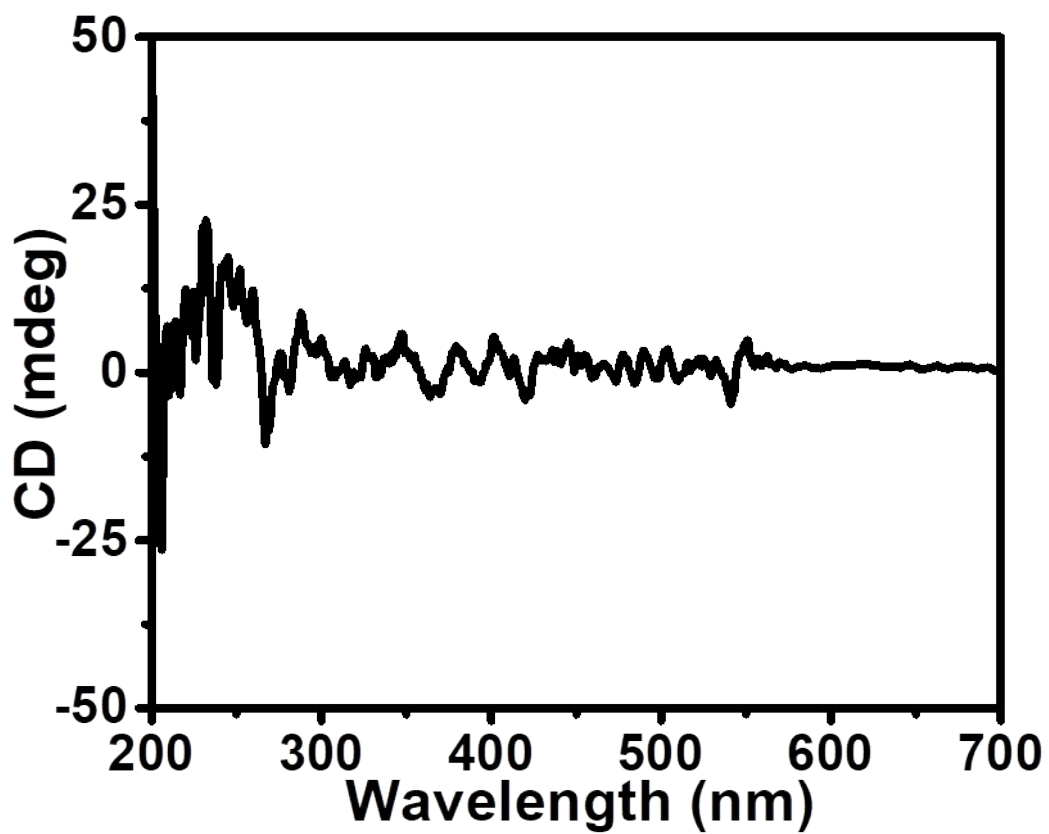
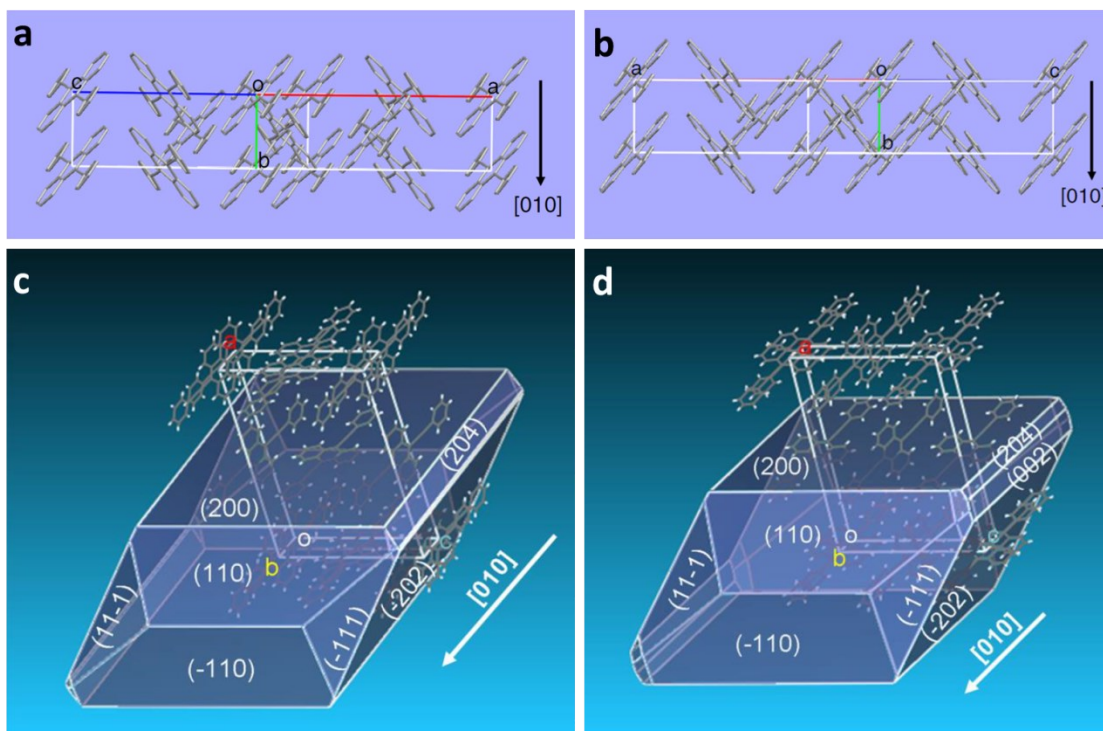
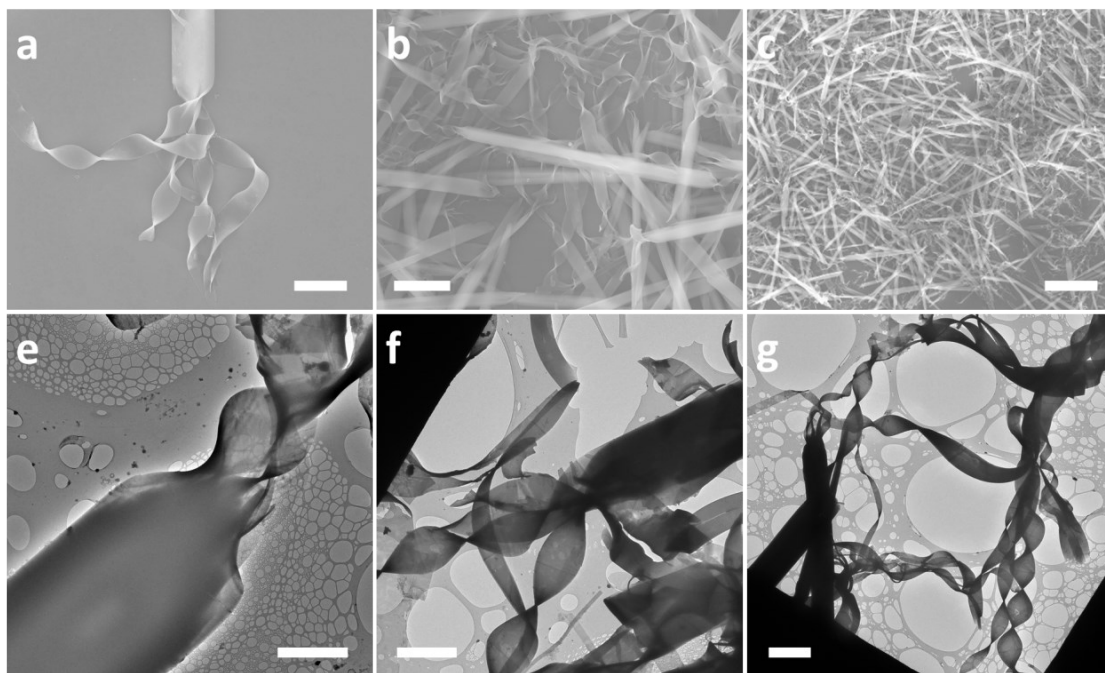


Figure S3. CD spectrum of the helical assembly  $BA_{0.72}BN_{0.28}$ .



**Figure S4.** Molecular packing of single crystals of BA (a) and BA<sub>x</sub>BN<sub>1-x</sub> alloy formed at mol/mol = 2:1 grown from DMF (b) along  $\pi$ - $\pi$  stacking directions; the predicted growth morphology and direction of BA crystal (c) and BA<sub>x</sub>BN<sub>1-x</sub> alloy formed at mol/mol = 2:1 grown from DMF (d) simulated by Material Studio based on the attachment energies. The data were obtained from the literature.<sup>1</sup>



**Figure S5.** SEM images of BA@BA<sub>0.72</sub>BN<sub>0.28</sub> core-shell structures prepared by adding 1mL stock solution of BA/BN ( $C_{BA} = 5$  mM,  $C_{BN} = 2.5$  mM) in THF with into a 5 mL of ethanol/H<sub>2</sub>O (v/v = 4:1) mixture with dispersion of BA rods as seeds. Scale bar: 5  $\mu$ m in **a**, 10  $\mu$ m in **b**, 50  $\mu$ m in **c**. TEM images of BA@BA<sub>0.72</sub>BN<sub>0.28</sub> core-shell structures prepared by the same process. Scale bar: 5  $\mu$ m in **e**, **f**, **g**.

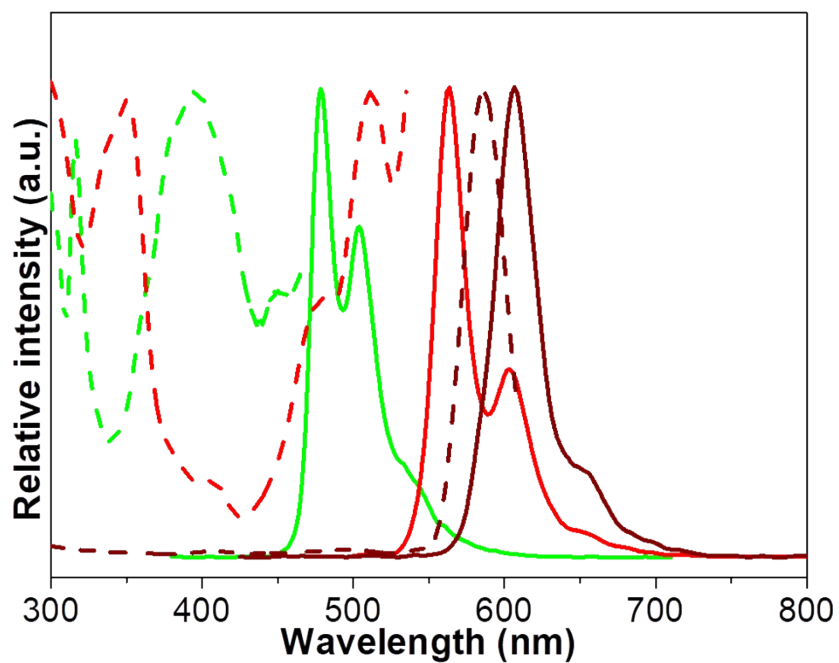


**Figure S6.** Excitation and emission spectra of BA solution (green curve,  $C_{BA}=10^{-4}$  mM in THF), BN solution (red curve,  $C_{BN}=10^{-4}$  mM in THF) and BA/BN precursor solution (wine curve,  $C_{BA} = 5$  mM,  $C_{BN} = 2.5$  mM in THF).

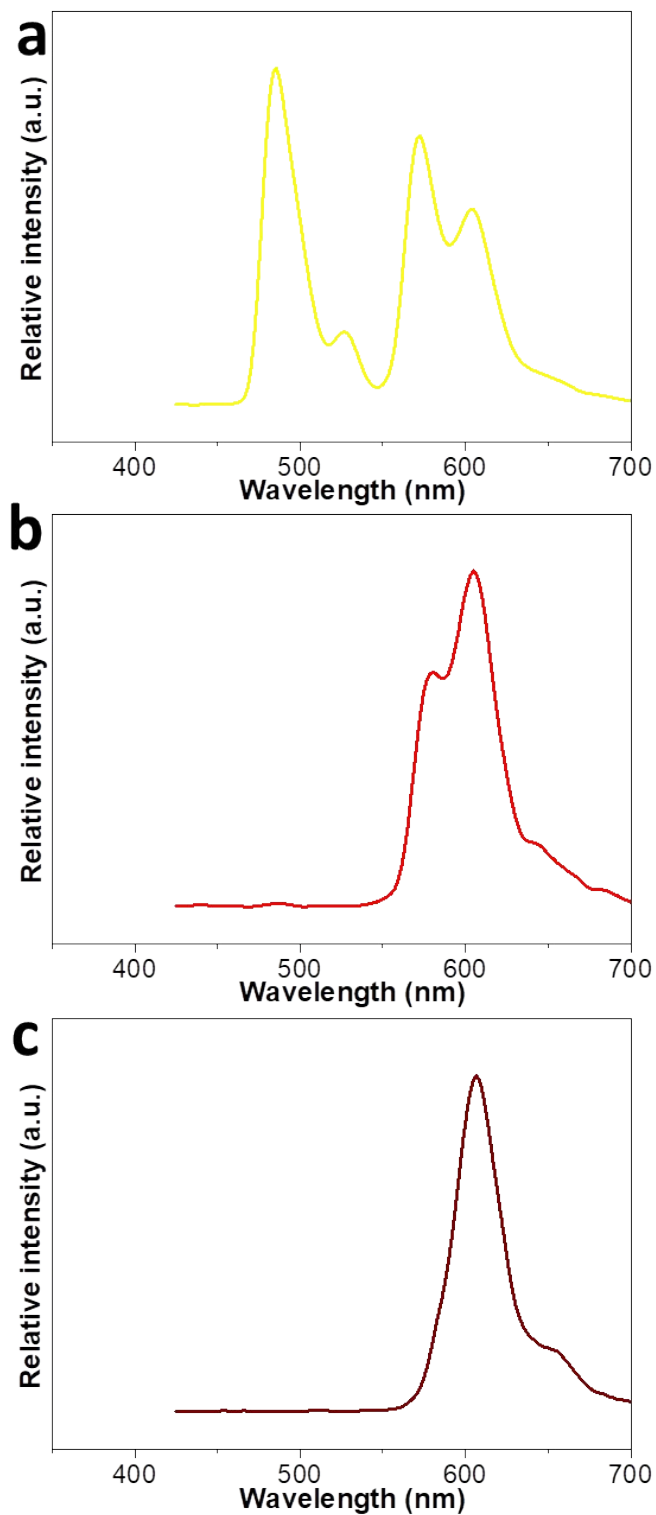


**Figure S7.** Emission spectra of BA/BN (mol/mol = 2:1) mixed solutions in THF with different concentrations (**a**,  $C_{\text{BA}} = 5 \times 10^{-4}$  mM and  $C_{\text{BN}} = 2.5 \times 10^{-4}$  mM, **b**,  $C_{\text{BA}} = 5 \times 10^{-2}$  mM and  $C_{\text{BN}} = 2.5 \times 10^{-2}$  mM, **c**,  $C_{\text{BA}} = 5$  mM and  $C_{\text{BN}} = 2.5$  mM).